Minimizing the Cross-Sectional Area and Maximizing Efficiency in Split-Input Two-Stage Gearboxes via NSGA-II with SAW-Guided Choice

Binh Duc Vu
Viet Tri University of Industry, Viet Tri City, Vietnam
vubinh@vui.edu.vn

Giang Ngoc Tran
Thai Nguyen University of Technology, Tich Luong Ward, Thai Nguyen City, Vietnam
tranngocgiang@tnut.edu.vn

Van Thanh Dinh
East Asia University of Technology, Trinh Van Bo Street, Hanoi City, Vietnam
thanh.dinh@eaut.edu.vn

Hien Thanh Bui
Thai Nguyen University of Technology, Tich Luong Ward, Thai Nguyen City, Vietnam
buithanhhienkc@tnut.edu.vn

Tam-Thi Do
Thai Nguyen University of Technology, Tich Luong Ward, Thai Nguyen City, Vietnam
dothitam@tnut.edu.vn (corresponding author)

Received: 19 September 2025 | Revised: 18 November 2025 and 10 December 2025 | Accepted: 11 December 2025

 DOI: https://doi.org/10.48084/etasr.14925

ABSTRACT

Split-input two-stage helical gearboxes must balance a compact footprint with high transmission efficiency. This study proposes a preference-aware multi-objective framework that couples NSGA-II with Simple Additive Weighting (SAW) to design split-input two-stage gearboxes under constraints. A parameterized gearbox model is formulated using the key design variables, including the first-stage gear ratio u_1 and the face-width coefficients of the first and second stages, X_{ba1} and X_{ba2}. The model is optimized with two objectives: minimizing the gearbox cross-sectional area A_c and maximizing the overall efficiency η_{gb}. For each target overall transmission ratio, u_h, NSGA-II is employed to generate the corresponding Pareto front, after which the SAW method ranks the non-dominated solutions based on user-specified preferences to identify a best-compromise design. The post-processing identified simple design rules: u_1 scales approximately linearly with u_h (fit $R^2 > 0.95$); X_{ba1} decreases with u_h and plateaus at its lower bound for higher u_h, while X_{ba2} remains nearly constant. The resulting fronts show the footprint–efficiency trade-off, and trend analysis demonstrates increasing area and slightly declining efficiency as u_h grows—guiding early sizing. The proposed NSGA-II + SAW workflow delivers reproducible, preference-aware selections and interpretable parametric relations, providing practical decision support for compact, high-efficiency split-input two-stage gearbox design.

Keywords-split-input two-stage gearbox; helical gearbox; multi-objective optimization; NSGA-II; Pareto front; SAW; cross-sectional area; gearbox efficiency

I. INTRODUCTION

Designing high-performance gear transmission units requires balancing conflicting objectives related to efficiency, volume, durability, and acoustic behavior. Multi-objective evolutionary algorithms (MOEAs) have become an essential method for addressing such trade-offs because they can efficiently explore complex, nonlinear design spaces and approximate the Pareto frontier. Authors in [1, 2] established MOEAs—particularly NSGA-II—as robust and widely adopted tools for engineering optimization. These methods have been successfully applied to various gearbox configurations, including multi-speed systems [3], helical and spur gear trains, and hybrid configurations [4], demonstrating their suitability for achieving balanced improvements in efficiency and structural performance. Recent applications further highlight the versatility of multi-objective optimization in gear design. Two-stage helical gearboxes have been optimized using statistical or hybrid methods [5], efficiency and transmission error reduction have been targeted [6], and noise and vibration reduction have been explored using multi-criteria tuning [7, 8]. Robust optimization approaches have also been proposed to accommodate uncertain load conditions [9]. Research has jointly minimized gearbox volume and improved efficiency for spur and helical gear pairs [10]. Decision-supported frameworks combining NSGA-II and Multi-Criteria Decision Making (MCDM) techniques—such as in spur gear systems [11, 12]—indicate the value of integrating optimization with a rational decision-selection step. Recently, studies on two-stage helical gearboxes have applied TOPSIS [13] or advanced ranking techniques [14] to select optimal designs from Pareto fronts. Parallel advances in related engineering fields emphasize the growing interest in sophisticated optimization and digital technologies, including metaheuristic reviews in scheduling [15] and industrial applications of digital twins [16].

Beyond conventional optimization, recent developments show a growing link between gearbox design and engineering approaches. In particular, digital twin technologies have gained attention for their ability to enhance real-time monitoring, predictive assessment, and virtual validation of mechanical systems. Authors in [17, 18] highlighted how digital twins are rapidly transforming fluid-power systems through improved diagnostics, data-driven optimization, and adaptive decision support. These insights reinforce the growing relevance of integrating advanced computational intelligence with mechanical system design, further motivating the development of transparent, optimization-driven frameworks such as the one proposed in the present study. Although these works demonstrate steady progress, three research gaps are yet to be addressed.

First, split-input two-stage helical gearboxes, where the first stage includes two parallel gear sets, have received limited attention despite their potential to distribute load more uniformly and reduce size. Existing studies have primarily focused on conventional two-stage or spur configurations. Second, although several MCDM approaches have been integrated with MOEAs, the SAW method—despite its transparency, monotonicity, and ability to integrate design preferences—has been rarely applied in gearbox optimization. Third, prior studies often emphasized final optimal points without conducting systematic parametric trend analysis, which is essential for understanding how key geometric variables evolve with gearbox size and efficiency. Within the broader MCDM domain, SAW has been applied successfully across diverse engineering scenarios, ranging from mechanical design evaluation to supplier selection and general multi-criteria ranking problems. Compared with TOPSIS, MARCOS, and other distance-based methods, SAW offers straightforward normalization, intuitive weighted aggregation, and minimal sensitivity to scale distortions, making it suitable for design environments requiring transparent trade-off reasoning. These characteristics support its integration into decision-supported gearbox optimization.

Motivated by these gaps, the present study develops a NSGA-II–based multi-objective optimization framework for a split-input two-stage helical gearbox, targeting simultaneous minimization of the cross-sectional area and efficiency maximization. A SAW-guided decision mechanism is incorporated to select representative optimal solutions from the Pareto set, and detailed parametric trends are analyzed to demonstrate how key gear parameters evolve as gearbox compactness varies. The novel contributions of the present study are:

- Formulation of a split-input two-stage helical gearbox model, incorporating geometric, strength, and efficiency constraints tailored to the dual-gear first stage.
- Development of a NSGA-II–based optimization framework for minimizing cross-sectional area and maximizing efficiency under practical design constraints.
- Integration of the SAW method as an interpretable decision-support tool, with justification based on its transparency and stable performance across engineering scenarios.
- Comprehensive parametric trend analysis revealing how gear ratios, facewidth factors, and load-sharing variables evolve with gearbox size.

II. OPTIMIZATION PROBLEM

A. Calculation of Gearbox Cross-Sectional Area

For a split-input two-stage helical gearbox, the cross-sectional area A_c is calculated using the schematics shown in Figure 1:

$$A_c = L \cdot H \quad (1)$$

where L and H are determined by:

$$L = d_{w11} + d_{w21}/2 + d_{w12}/2 + d_{w22} + 4 \cdot \delta \quad (2)$$

$$H = max\ (d_{w21}, d_{w22}) + 8.5 \cdot \delta \quad (3)$$

where δ =7 to 10 mm [18] and d_{w1i}, d_{w2i} (i = 1, 2) are the pitch diameters of the pinion and the gear of stage *i,* which can be determined by [19]:

$$d_{w1i} = 2 \times \left(\frac{a_{wi}}{u_i+1}\right) \quad (4)$$

$$d_{w1i} = 2 \times \left(\frac{a_{wi} \times u_i}{u_i + 1}\right) \quad (5)$$

where a_{wi} (i = 1, 2) is the center distance of stage i, which can be computed using [19]:

$$a_{wi} = k_a \cdot (u_i + 1) \cdot \sqrt[3]{T_{1i} \cdot k_{H\beta} / ([AS_i]^2 \cdot u_i \cdot X_{bai})} \quad (6)$$

where X_{bai} is the wheel face width coefficient of stage i^{th} and T_{1i} (i =1, 2) is the pinion torque of stage i, which is computed using:

$$T_{11} = \frac{T_r}{2 \cdot u_{gb} \cdot \eta_{hg}^2 \cdot \eta_{be}^3} \quad (7)$$

$$T_{12} = \frac{T_r}{u_2 \cdot \eta_{hg} \cdot \eta_{be}^2} \quad (8)$$

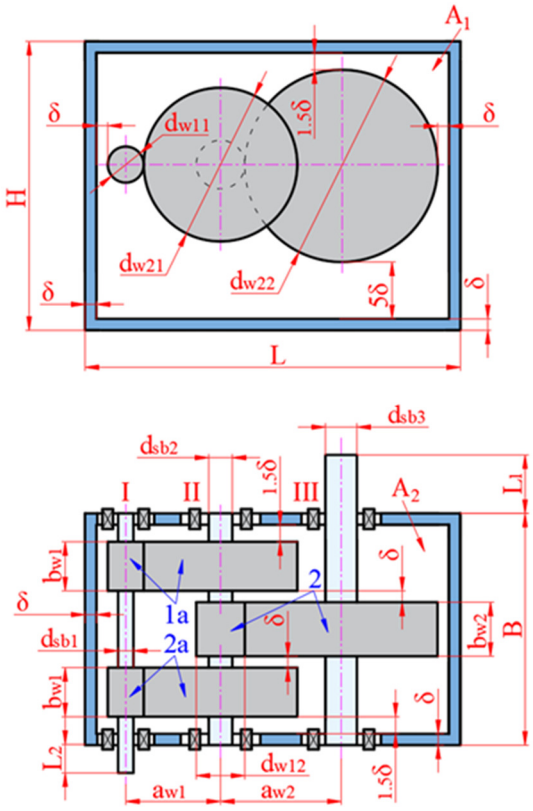

Fig. 1. Schematic for the determination of the cross-sectional area.

B. Calculation of Gearbox Efficiency

The total efficiency of the gearbox, η_{gb}, is calculated by:

$$\eta_{gb} = 100 - \frac{100 \cdot P_l}{P_{in}} \quad (9)$$

where P_l denotes the total power loss in the gearbox and P_{in} is the input gearbox power. P_l is determined by [20]:

$$P_l = P_{lg} + P_{lb} + P_{ls} + P_{Z0} \quad (10)$$

where P_{lg}, P_{lb}, P_{ls}, and P_{Z0} are the gear meshing loss, bearing friction loss, seal resistance loss, and loss due to idle motion, respectively. These parameters were found as proposed in [5].

C. Objective Functions and Constraints

The split–first-stage two-stage helical gearbox is formulated as a bi-objective optimization problem that simultaneously targets a compact footprint and high transmission efficiency. The footprint is quantified in terms of the cross-sectional area A_c, while performance is measured by the overall efficiency η_{gb}. The objective functions are:

$$minf_1 = A_c \quad (11)$$

$$maxf_2 = \eta_{gb} \quad (12)$$

To guarantee feasibility and manufacturability, the decision variables—namely the stage gear ratios u_i and the face-width coefficients X_{bai} (for each stage i)—are restricted to the following practical limits [19] :

$$1 \leq u_i \leq 9 \quad (13)$$

$$0.25 \leq X_{bai} \leq 0.4 \quad (14)$$

III. OPTIMIZATION METHODOLOGY

A. NSGA-II–Based Multi-Objective Optimization

The split–first-stage two-stage helical gearbox is defined by the stage gear ratios u_i and the face-width coefficients X_{bai} (for i =1, 2). The two conflicting objectives are the cross-sectional area A_c to be minimized and the overall efficiency η_{gb} to be maximized, as already stated in (11) and (12). Practical feasibility and manufacturability are enforced by the bound constraints as defined in (13) and (14). The steps of the NSGA-II optimization algorithm are:

- Initialization: Randomly sample a population within (13)–(14), compute the derived geometric quantities needed to evaluate A and η_{gb}.
- Evaluation: For each individual, evaluate $(f_1, f_2) = (A_c, -\eta_{gb})$ (the minus sign permits a bi-objective minimization casting).
- Non-dominated sorting: Rank individuals into Pareto fronts f_1, f_2, by dominance depth.
- Diversity preservation: Compute the crowding distances within each front.
- Selection, crossover, mutation: Use binary tournament on (rank, crowding) to form a mating pool, apply simulated binary crossover and polynomial mutation (probabilities and distribution indexes set per standard practice).
- Elitist replacement: Merge parents and offspring, reapply non-dominated sorting, and truncate by rank and crowding to a fixed population size.
- Termination: Iterate until a maximum number of generations is reached or convergence (e.g., hypervolume change) is below a threshold.

The algorithm returns a Pareto set of non-dominated gearbox designs for each u_h. These sets feed the decision-making stage are described below.

B. Pseudocode of the Integrated NSGA-II

The NSGA-II algorithm is employed to generate Pareto-optimal gearbox designs for each prescribed overall transmission ratio u_h. The decision vector is $x = [u_1, X_{ba1}, X_{ba2}]$, and each candidate produces the second-stage ratio $u_2 = u_h/u_1$. The gearbox model evaluates the cross-sectional area $A_c$and overall efficiency η_{gb}.

1) Algorithm 1. NSGA-II-Based Multi-Objective Optimization (Short Form)

1. Inputs: Bounds of u_1, X_{ba1}, X_{ba2}; overall ratios $\{u_h\}$; N, G; SBX and mutation parameters.
2. Output: Pareto set $\mathcal{P}(u_h)$for each u_h.
3. For each overall transmission ratio u_h:

- Initialize population
- Generate N individuals within bounds.
- Evaluate individuals
- Compute $u_2 = u_h/u_1$; penalize if infeasible.
- Compute objectives $[A_c, -\eta_{gb}]$.

4. For generation $g = 1$ to G:

- Apply non-dominated sorting and assign ranks.
- Compute crowding distances.
- Select parents via binary tournament.
- Generate offspring via SBX crossover + polynomial mutation.
- Evaluate offspring and form the next generation using elitist replacement.

5. Extract the final Pareto front:

- Set $\mathcal{P}(u_h)$= first non-dominated front.

The obtained Pareto sets are later processed using the SAW-based MCDM method to select representative compromise designs.

C. SAW-Based Multi-Criteria Decision Making

In this work, the MCDM problem was resolved with the SAW approach. To accurately implement the SAW technique, it is essential to meticulously monitor the subsequent processes [21]:

Create the first decision-making matrix:

$$X = \begin{array}{c|cccc} & C_1 & C_2 & \cdots & C_n \\ \hline A_1 & y_{11} & y_{12} & \cdots & y_{1n} \\ A_2 & y_{21} & y_{22} & \cdots & y_{2n} \\ \vdots & \vdots & \vdots & \ddots & \vdots \\ A_m & y_{m1} & y_{m2} & \cdots & y_{mn} \end{array} \quad (15)$$

where m and n are options and criterion numbers.

Compute the normalized matrix by:

$$n_{ij} = \frac{r_{ij}}{maxr_{ij}} \quad (16)$$

$$n_{ij} = \frac{minr_{ij}}{r_{ij}} \quad (17)$$

Equation (16) is used for the gearbox efficiency target, while (17) is used for the cross-sectional area.

Determine the preference value for each option:

$$V_i = \sum_{j=1}^{n} w_j \cdot n_{ij} \quad (18)$$

Rank the alternative's order by maximizing V_i.

IV. RESULTS AND DISCUSSIONS

A. Pareto Landscape and the A_c–η_{gb} Trade-Off

Figure 2 shows the Pareto fronts obtained by NSGA-II for a set of overall ratios u_h, under the objectives of (12) and (13) and limits of (14) and (15). Each colored curve represents the best non-dominated compromises between the cross-sectional area A_c (to be minimized) and gearbox efficiency η_{gb} (to be maximized) at a fixed u_h. For every u_h, the front shows a typical diminishing-return behavior: moving rightward (larger A_c) yields progressively smaller gains in η_{gb}. The left end of each front corresponds to compact designs, where A_c is limited primarily by the geometric/strength requirements and the lower bound of face-width coefficients (15); the right end corresponds to wider gears and larger supporting sections that reduce losses and slightly raise η_{gb}. The curvature creates a knee region-a short arc where a modest increase in A_c still delivers a relatively large improvement in η_{gb}. This knee is the most attractive zone for balanced preferences and is the focus of the SAW selection.

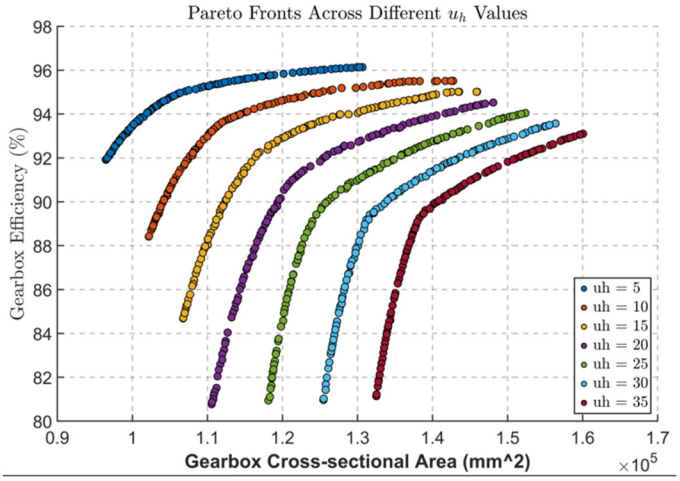

Fig. 2. Pareto fronts of gearbox efficiency versus cross-sectional area with different u_h.

1) Effect of the Overall Ratio u_h.

Comparing fronts across colors shows a clear, monotonic shift with u_h:

- As u_h increases, the entire front moves to the right (larger Ac) and downward (lower η_{gb}), indicating that higher transmission ratios inherently demand a larger footprint and incur additional losses.
- For the same target efficiency, the required A_c grows with uh; conversely, at a fixed A_c, the achievable η_{gb} decreases when u_h is higher.
- For high uh, with X_{ba1} constrained by the lower bound (15), the footprint cannot be reduced further, and the marginal improvement in η_{gb} from increased widths becomes negligible.

2) Implications

These fronts provide a quantitative map of the trade-off between footprint and efficiency at design-time. They allow designers to: (i) locate minimum-footprint solutions (left ends) when space is critical; (ii) target high-efficiency solutions (upper right) when losses dominate the specification; and (iii) identify best-compromise designs near the knee before applying the SAW ranking. The aggregated tendency—A_c increasing and η_{gb} slightly decreasing with u_h—is consistent with the mean trends reported later in Figure 4, reinforcing the robustness of the trade-off patterns produced by the NSGA-II search.

B. SAW Ranking and Best-Compromise Selections

Based on the data of all the Pareto fronts, the non-dominated solutions at each fixed u_h are assembled into the decision matrix X in (15), where the benefit criterion is efficiency η_{gb} and the cost criterion is cross-sectional area A_c. Linear normalization follows (16) and (17), with (16) applied to η_{gb} and (17) to A_c, and the preference score of each alternative is computed by (18). The weights of the criteria are determined by the entropy method. Alternatives are ranked by maximizing V_i.

TABLE I. SAW-SELECTED BEST-COMPROMISE DESIGNS FOR DIFFERENT u_h

u_h	u_1	X_{ba1}	X_{ba2}	A_c (mm^2)	η_{gb} (%)
5	3.56	0.40	0.40	96469.00	91.92
10	5.56	0.36	0.40	103134.82	89.26
15	6.82	0.31	0.40	111860.08	89.71
20	8.02	0.29	0.40	117690.74	88.98
25	9.00	0.25	0.40	123976.81	89.11
30	9.00	0.25	0.40	131181.49	89.18
35	9.00	0.25	0.40	138255.67	89.27

Table I reports, for each u_h, the selected non-dominated design along with its decision variables (u_1, X_{ba1}, and X_{ba2}) and objectives (A_c, η_{gb}). Across the studied ratios, the SAW selections represent balanced trade-offs between footprint and efficiency on the corresponding Pareto fronts. As u_h increases, the chosen designs exhibit the same global tendencies seen in Figure 4: A_c rises while η_{gb} declines slightly, quantifying the footprint cost of sustaining acceptable efficiency at higher overall ratios.

1) Implications for Design Variables

The SAW-selected points are consistent with the parametric relations: (i) the stage-1 ratio u_1 varies nearly linearly with u_h, as illustrated in Figure 5; (ii) the X_{ba1} decreases with u_h and becomes active at its lower limit of 0.25 for larger u_h (constraint (15)), whereas X_{ba2} remains nearly constant at a high level. Once X_{ba1} is bound-limited, further reductions of first-stage face-width are infeasible. Consequently, total A_c tends to increase to maintain satisfactory η_{gb} as u_h increases.

C. Global Trends Versus u_h

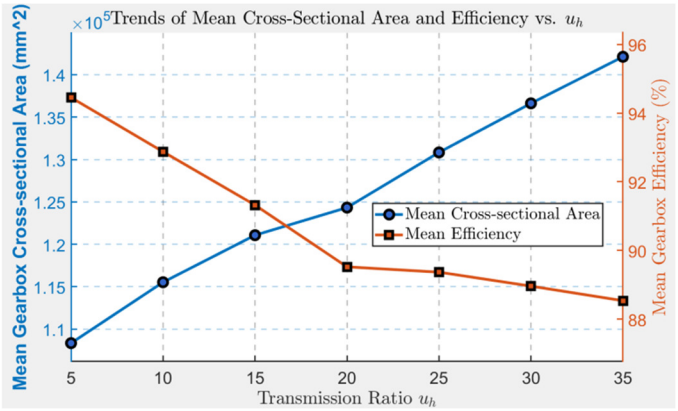

Fig. 3. Global trends versus u_h for mean cross-sectional area and mean efficiency.

1) Key Observations from Figure 3

- A_c increases nearly linearly with u_h; the slope is fairly uniform across the studied range, implying progressively larger mounting space/baseplate requirements at higher ratios.
- η_{gb} decreases monotonically with u_h and plateaus at high u_h: the initial penalty is sizable, then the marginal loss diminishes—i.e., a classic diminishing-returns pattern.

2) Mechanical Interpretation

Even though X_{ba1} decreases and may plateau at its lower limit, overall A_c still grows because: (i) the center distance and pitch radii increase with ratio and strength constraints, and (ii) the housing/shaft/bearing sections require reinforcement to maintain stiffness and life as branch torques rise. Efficiency declines because higher u_h elevates sliding velocity and frictional losses at the tooth contacts, alongside higher bearing and churning losses. Beyond a certain size, further increase in width or sectional area yields marginal efficiency gains, producing the observed flattening.

3) Design Implications

- With tight footprint constraints, favor low-to-mid u_h.
- If efficiency is prioritized, accept a larger A_c (move rightward along the front) to obtain higher η_{gb}.
- Mid-range u_h often delivers balanced trade-offs, aligning with the SAW-selected knees.

Overall, the mean trends of A_c and η_{gb} versus u_h reinforce the Pareto patterns, as displayed in Figure 2, and are consistent with the parametric rules (near-linear $u_1 \sim u_h$; X_{ba1} decreasing then saturating; X_{ba2} approximately constant). These results provide quantitative guidance for early sizing and configuration selection under explicit preferences.

D. Parametric Relations of First-Stage Design Variables

1) Relation between u_1 and u_h

Figure 4 shows the relation between the optimal gear ratio of stage-1 u_1 and u_h. The regression results and the SAW selections indicate a piecewise rule: linear at low–mid u_h, and saturation at the upper limit when u_h is sufficiently large. Specifically, $u_h \leq 23.6$ (with R^2=0.9891):

$$u_1 = 0.2868 \cdot u_h + 2.3878 \quad (19)$$

If $u_h \geq 23.6$, then $u_1 = 9$, where 9 is the upper limit of u_1 according to the design constraint in (13).

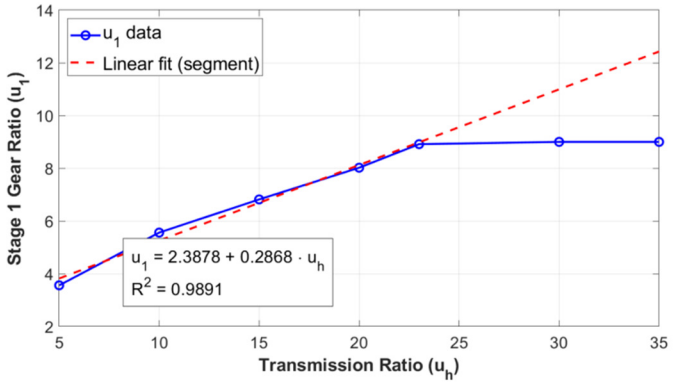

Fig. 4. Parametric relation between optimal gear ratio of stage-1 u_1 and u_h.

2) Evolution of X_{ba1} and X_{ba2} Versus u_h

Regression indicates a piecewise trend for X_{ba1} with a transition near $u_h = 25$: a linear decline at low–mid u_h followed by saturation at the lower bound at higher u_h, with $R^2 = 0.9521$:

$$X_{ba1} = \begin{cases} 0.4204 - 0.0063 \cdot u_h \; if \; u_h \leq 25 \\ 0.25 \; if \; u_h \geq 25 \end{cases} \quad (20)$$

where 0.25 is the lower limit from constraint (14), as seen in Figure 5. Specifically, for $u_h \leq 25$, the relative face width at stage-1 can be gradually reduced to save footprint while maintaining performance; once $u_h \approx 25$, the lower-limit constraint becomes active, and X_{ba1} plateaus at 0.25.

In contrast, X_{ba2} remains constant at a high level across the explored range ($X_{ba2} = 0.4$), reflecting the need to preserve stiffness, favorable contact stress, and lower losses at stage-2 as branch load increases. Together, the piecewise rule for X_{ba1} and the stability of X_{ba2} explain the global trend seen earlier: at larger u_h, with X_{ba1} already bound-active, the footprint (via A_c) tends to increase to sustain η_{gb}; at moderate u_h, a judicious width allocation between the two stages still yields noticeable efficiency gains at a moderate footprint cost. These trends illustrate how load distribution and structural design requirements evolve with the gearbox's overall ratio.

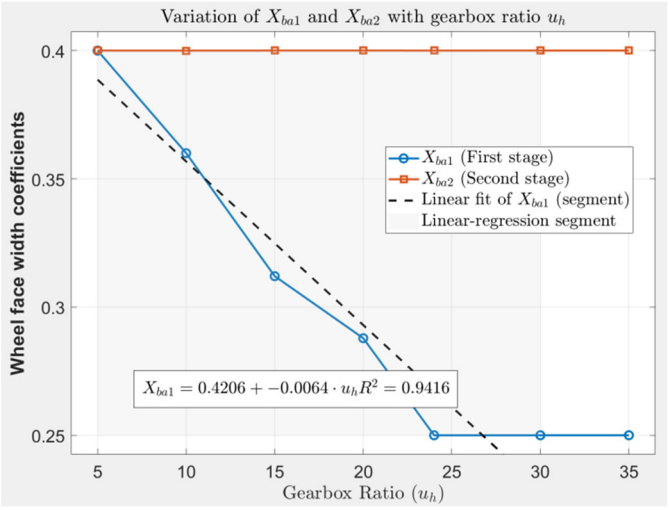

Fig. 5. Evolution of X_{ba1} and X_{ba2} with u_h.

V. CONCLUSIONS

This study proposed an NSGA-II–based optimization framework for a split-input two-stage helical gearbox and introduced a Simple Additive Weighting (SAW)-based decision-making step to select designer-preferred solutions. Compared with existing gearbox optimization studies, the work contributes a distinct objective formulation focusing on minimizing the gearbox cross-sectional area and maximizing efficiency, together with a systematic parametric trend analysis across different overall transmission ratios. The integration of NSGA-II with an explicit Multi-Criteria Decision Making (MCDM) step represents the methodological novelty, offering clearer and more transparent compromise selection compared to traditional optimization-only approaches.

The study has several limitations, including considering only two objectives, the constraints were treated deterministically, and efficiency evaluation relied solely on analytical models without experimental validation. Future works should address these limitations by incorporating robustness or uncertainty analysis, validating the results experimentally or through high-fidelity simulations, and comparing the SAW-based selection with alternative MCDM methods such as TOPSIS, MARCOS, or AHP.

ACKNOWLEDGMENT

This work was supported by Thai Nguyen University of Technology, Vietnam.

REFERENCES

[1] C. A. Coello Coello, D. A. Van Veldhuizen, and G. B. Lamont, *Evolutionary Algorithms for Solving Multi-Objective Problems*, 2nd ed. New York City, NY, USA: Springer New York, 2002.

[2] K. Deb, A. Pratap, S. Agarwal, and T. Meyarivan, "A Fast and Elitist Multiobjective Genetic Algorithm: NSGA-II," *IEEE Transactions on Evolutionary Computation*, vol. 6, no. 2, pp. 182–197, Apr. 2002, https://doi.org/10.1109/4235.996017.

[3] K. Deb and S. Jain, "Multi-Speed Gearbox Design using Multi-Objective Evolutionary Algorithms," *Journal of Mechanical Design*, vol. 125, no. 3, pp. 609–619, Sept. 2003, https://doi.org/10.1115/1.1596242.

[4] M. Mendez, D. A. Rossit, B. Gonzalez, and M. Frutos, "Proposal and Comparative Study of Evolutionary Algorithms for Optimum Design of

a Gear System," *IEEE Access*, vol. 8, pp. 3482–3497, 2020, https://doi.org/10.1109/ACCESS.2019.2962906.

[5] X.-H. Le and N.-P. Vu, "Multi-Objective Optimization of a Two-Stage Helical Gearbox using Taguchi Method and Grey Relational Analysis," *Applied Sciences*, vol. 13, no. 13, June 2023, Art. no. 7601, https://doi.org/10.3390/app13137601.

[6] E. B. Younes, C. Changenet, J. Bruyère, E. Rigaud, and J. Perret-Liaudet, "Multi-Objective Optimization of Gear Unit Design to Improve Efficiency and Transmission Error," *Mechanism and Machine Theory*, vol. 167, Jan. 2022, Art. no. 104499, https://doi.org/10.1016/j.mechmachtheory.2021.104499.

[7] Y. Lei, L. Hou, Y. Fu, J. Hu, and W. Chen, "Research on Vibration and Noise Reduction of Electric Bus Gearbox Based on Multi-Objective Optimization," *Applied Acoustics*, vol. 158, Jan. 2020, Art. no. 107037, https://doi.org/10.1016/j.apacoust.2019.107037.

[8] L. Qi, J. Zhou, and H. Xu, "Multi-Objective Optimization of Gearbox Based on Panel Acoustic Participation and Response Surface Methodology," *Journal of Low Frequency Noise, Vibration and Active Control*, vol. 41, no. 3, pp. 1108–1130, Sept. 2022, https://doi.org/10.1177/14613484221091075.

[9] S. Salomon, G. Avigad, R. C. Purshouse, and P. J. Fleming, "Gearbox Design for Uncertain Load Requirements using Active Robust Optimization," *Engineering Optimization*, vol. 48, no. 4, pp. 652–671, Apr. 2016, https://doi.org/10.1080/0305215X.2015.1031659.

[10] D. Miler, D. Žeželj, A. Lončar, and K. Vučković, "Multi-Objective Spur Gear Pair Optimization Focused on Volume and Efficiency," *Mechanism and Machine Theory*, vol. 125, pp. 185–195, July 2018, https://doi.org/10.1016/j.mechmachtheory.2018.03.012.

[11] E. S. Maputi and R. Arora, "Multi-Objective Optimization of a 2-Stage Spur Gearbox using NSGA-II and Decision-Making Methods," *Journal of the Brazilian Society of Mechanical Sciences and Engineering*, vol. 42, no. 9, Sept. 2020, Art. no. 477, https://doi.org/10.1007/s40430-020-02557-2.

[12] Q. Yao, "Multi-Objective Optimization Design of Spur Gear Based on NSGA-II and Decision Making," *Advances in Mechanical Engineering*, vol. 11, no. 3, Mar. 2019, Art. no. 1687814018824936, https://doi.org/10.1177/1687814018824936.

[13] H.-D. Tran, V.-T. Dinh, D.-B. Vu, D. Vu, A.-T. Luu, and N. P. Vu, "Application of the TOPSIS Method for Multi-Objective Optimization of a Two-Stage Helical Gearbox," *Engineering, Technology & Applied Science Research*, vol. 14, no. 4, pp. 15454–15463, Aug. 2024, https://doi.org/10.48084/etasr.7551.

[14] T. Q. Hung, V. D. Binh, D. V. Thanh, L. A. Tung, and N. K. Tuan, "Multi-Objective Optimization of a Two-Stage Helical Gearbox with Two Gear Sets in First Stage to Reduce Volume and Enhance Efficiency using the EAMR Technique," *Engineering, Technology & Applied Science Research*, vol. 15, no. 1, pp. 19288–19294, Feb. 2025, https://doi.org/10.48084/etasr.9224.

[15] D. C. Hajariwala, S. S. Patil, and S. M. Patil, "A Review of Metaheuristic Algorithms for Job Shop Scheduling," *Engineering Access*, vol. 11, no. 1, Jan. 2025.

[16] A. D. Khamkar and S. M. Patil, "Digital Twin in Fluid Power: Reviewing Constituents," *International Research Journal of Multidisciplinary Scope*, vol. 05, no. 01, pp. 750–765, 2024, https://doi.org/10.47857/irjms.2024.v05i01.0365.

[17] A. D. Khamkar and S. M. Patil, "Digital Twin in Fluid Power: Review-Technology Trends," *International Research Journal of Multidisciplinary Scope*, vol. 05, no. 02, pp. 596–610, 2024, https://doi.org/10.47857/irjms.2024.v05i02.0586.

[18] A. D. Khamkar and S. M. Patil, "Digital Twin in Fluid Power: Review - Uses and Outlook," *International Research Journal of Multidisciplinary Scope*, vol. 05, no. 03, pp. 79–96, 2024, https://doi.org/10.47857/irjms.2024.v05i03.01085.

[19] T. Chat and U. L. Van, *Design and Calculation of Mechanical Transmissions Systems*, vol. 1. Hanoi, Vietnam: Educational Republishing House, 2007.

[20] D. Jelaska, *Gears and Gear Drives*, 1st ed. Hoboken, NJ, USA: John Wiley & Sons, 2012.

[21] K. Sri. S. Hartati, S. Harjoko, and R. Wardoyo, *Fuzzy Multi-Attribute Decision Making (Fuzzy MADM)*. Yogyakarta, Indonesia: Graha Ilmu, 2006.